SPANDIDOS PUBLICATIONS

ONCOLOGY REPORTS 26: 843-851, 2011

Cilengitide inhibits metastatic bone colonization in a nude rat model

MAREN BRETSCHI[1], MAXIMILIAN MERZ[1], DORDE KOMLJENOVIC[1], MARTIN R. BERGER[2], WOLFHARD SEMMLER[1] and TOBIAS BÄUERLE[1]

[1]Department of Medical Physics in Radiology, and [2]Chemotherapy and Toxicology Unit, German Cancer Research Center, 69120 Heidelberg, Germany

Received April 13, 2011; Accepted May 16, 2011

DOI: 10.3892/or.2011.1373

Abstract. Integrins $\alpha_v\beta_3$ and $\alpha_v\beta_5$ are considered to play an important role in the pathogenesis of breast cancer bone metastases. This study investigates the effects of the $\alpha_v\beta_3/\alpha_v\beta_5$ integrin-specific inhibitor cilengitide during early metastatic bone colonization. The impact of cilengitide on the migration, invasion and proliferation of MDA-MB-231 human breast carcinoma cells as well as on bone resorption by osteoclasts was investigated *in vitro*. For *in vivo* experiments, nude rats were treated with cilengitide for 30 days starting one day after site-specific tumor cell inoculation in the hind leg, and the course of metastatic changes in bone was followed using flat-panel volumetric computed tomography (VCT) and magnetic resonance imaging (MRI). Vascular changes in bone metastases were investigated using dynamic contrast-enhanced (DCE-) MRI-derived parameters amplitude A and exchange rate coefficient k_{ep}. *In vitro*, cilengitide treatment resulted in a decrease in proliferation, migration and invasion of MDA-MB-231 cells, as well as of osteoclast activity. *In vivo*, the development of bone metastasis in the hind leg of rats was not prevented by adjuvant cilengitide treatment, but cilengitide reduced the volumes of osteolytic lesions and respective soft tissue tumors of developing bone metastases as assessed with VCT and MRI, respectively. DCE-MRI revealed significant changes in the A and k_{ep} parameters including decreased relative blood volume and increased vessel permeability after cilengitide treatment indicating vessel remodeling. In conclusion, during early pathogenic processes of bone colonization, cilengitide treatment exerted effects on tumor cells, osteoclasts and vasculature reducing the skeletal lesion size of experimental skeletal metastases.

Correspondence to: Dr Tobias Bäuerle, Department of Medical Physics in Radiology, German Cancer Research Center, Im Neuenheimer Feld 280, 69120 Heidelberg, Germany
E-mail: t.baeuerle@dkfz.de

Key words: bone metastases, breast cancer, adjuvant treatment, cilengitide, integrins $\alpha_v\beta_3$ and $\alpha_v\beta_5$, dynamic contrast-enhanced magnetic resonance imaging, volumetric computed tomography

Introduction

Metastasis is a common finding during malignant tumor disease and is the major cause of death in women with breast cancer. Bone metastases occur in approximately 70% of breast cancer patients and cause severe complications including pathological bone fracture, bone pain, hypercalcemia and spinal cord compression (1). Adjuvant treatment options for inhibiting breast cancer bone metastases are currently limited to hormone therapy, chemotherapy and bisphosphonates. Although these drugs are administered to decrease the number and size of developing bone metastases, their use may be limited due to severe side effects or non-responsiveness (2-4). It is therefore crucial to understand the factors that regulate pathogenic processes in the establishment of bone metastases and to develop new and more effective therapies.

Members of the integrin family influence several aspects of tumor progression and metastasis. Specific integrins such as $\alpha_v\beta_3$ and $\alpha_v\beta_5$ are involved in regulating migration, invasion and proliferation of osteotropic tumor cells as well as bone colonization and angiogenesis induced by metastasized cells. $\alpha_v\beta_3$ and $\alpha_v\beta_5$ integrins were shown to influence these processes by mediating interactions with extracellular matrix (ECM) proteins, e.g. bone sialoprotein (BSP), through the arginine-glycine-aspartic acid (RGD) motif and matrix metalloproteinase-2 (MMP-2) in promoting osteotropic cancer cell invasion (5-8). In tumor-induced angiogenesis, $\alpha_v\beta_3$ and $\alpha v\beta_5$ integrins are up-regulated on activated endothelial cells, and are involved in the initiation of new vessel formation, endothelial cell survival and vascular permeability (9,10). Osteoclasts also express $\alpha_v\beta_3$ integrin to facilitate migration, adhesion to bone, and resorption of the bone matrix (11). The preventive treatment of animals bearing MDA-MB-435 breast cancer cells with a peptidomimetic inhibitor of $\alpha_v\beta_3$ was shown to reduce bone destruction (12).

Cilengitide (EMD 121974) is a small cyclic RGD-containing pentapeptide that selectively inhibits $\alpha_v\beta_3$ and $\alpha_v\beta_5$ integrins (13-15). Cilengitide acts on $\alpha_v\beta_3/\alpha_v\beta_5$-expressing tumor cells, depriving them of signals needed for survival and proliferation, which results in the inhibition of angiogenesis and tumor growth (15-17). In late-stage clinical trials, cilengitide exerted anti-tumor effects in glioblastoma multiforme and demonstrated a good safety profile (18,19).

Recently, we demonstrated that the inhibition of $\alpha_v\beta_3/\alpha_v\beta_5$ integrins by cilengitide reduced bone resorption and soft tissue tumor growth in well-established experimental breast cancer bone metastases (20). However, the effect of the inhibition of $\alpha_v\beta_3/\alpha_v\beta_5$ integrins during the processes of bone colonization by breast cancer cells is unknown, i.e. in an adjuvant treatment setting. To examine whether therapeutic targeting of $\alpha_v\beta_3/\alpha_v\beta_5$ integrins by cilengitide impedes bone metastasis formation, we first investigated the effects of cilengitide on the migration, invasion and proliferation of MDA-MB-231 human breast cancer cells and on osteoclast activity *in vitro*. Furthermore, we studied the effects of adjuvant cilengitide treatment *in vivo* assessing tumor growth, bone resorption and angiogenesis of developing skeletal metastases in nude rats by non-invasive imaging techniques.

Materials and methods

In vitro assays

Migration assay. A model for cell migration was used to characterize the metastatic ability of MDA-MB-231 cells in the presence of cilengitide. The migration assay consisted of two compartments. The bottom layer (24-well plate, Nunc) was utilized to stimulate and take up those cells which were to migrate through the pores of a polycarbonate filter membrane (pore size 8 μm; upper layer) as previously described with the following minor modifications (21,22). MDA-MB-231 cells ($1x10^4$) (purchased from ATCC and cultivated under standard conditions) were incubated with cilengitide (EMD 121974; Merck, Darmstadt, Germany) at concentrations ranging from 1-200 μg/ml (1.7-340 μM). The bottom layer was filled with 0.5 ml conditioned media from SAOS-2 osteosarcoma cells as a chemoattractant instead of SAOS-2 osteosarcoma cells. The polycarbonate filter was removed from the bottom chamber after 24, 48 and 72 h of cultivation and transferred onto a fresh bottom chamber well. Cells migrating through the pores into the bottom layer were counted daily for four days using an inverted microscope.

Invasion assay. Cell culture inserts (24-well) with 8-μm pores were coated with a thin layer of collagen type I solution prepared as follows: 8 volumes of ice-cold collagen solution (4 mg/ml in 0.1% acetic acid) and 1 volume of 10X Hanks' buffered saline were neutralized with NaOH as previously described (23). MDA-MB-231 cells (10^5) suspended in 1 ml RPMI-1640 medium were plated onto the upper compartment of a transwell chamber. The lower chamber was filled with 1 ml RPMI-1640 medium. MDA-MB-231 cells were incubated with cilengitide or RPMI-1640 medium alone for 5 days with cilengitide at concentrations of 1-200 μg/ml. After incubation for 1, 3 and 5 days, filters were then washed with PBS, and the non-invading cells that remained on the upper surface of the filter were removed with a cotton swab. Invading cells were fixed in 80% ethanol for 30 min and stained with Meyer's Hemalaun solution for 3 h. These invaded cells were visualized and counted from six randomly selected fields of view under an inverted microscope.

Proliferation assay. RPMI medium (100 μl per well) containing $5x10^3$ MDA-MB-231 cells was seeded onto 96-well plates (Microtest™, Becton-Dickinson, Heidelberg, Germany) as previously described (22). After 24 h, 100 μl medium was added which contained cilengitide (1-200 μg/ml). The plates were cultured for 1-5 days, and then 10 μl/well of 3-[4,5-dimethylthiazol-2-yl]-2,5-diphenyltetrazolium bromide (MTT; 10 mg/ml) was added. The supernatant was removed after 3 h of incubation, and the formazan crystals that developed were dissolved by adding 100 μl acidified 2-propanol/well (0.04 N HCl). Extinction was measured by an automated microtiter plate reader at 540 nm, reference filter 690 nm (Multiscan FC, Thermo Fisher Scientific Oy, Vantaa, Finland).

Bone resorption assay. A 96-well OsteoLyse™ cell culture plate (Lonza, Walkersville, MD, USA) coated with fluorophore-derivatized human bone matrix (europium-conjugated collagen) was used. Primary osteoclast precursors (BioCat, Heidelberg, Germany) were seeded onto the cell culture plate in medium containing M-CSF (macrophage colony-stimulating factor) and soluble RANKL (receptor activator of nuclear factor κB ligand). After 5 days of differentiation, osteoclasts were cultured for 5 days and treated with cilengitide (1-200 μg/ml). The resorptive activity of the osteoclasts, as reflected by the release of europium-labelled collagen fragments, was measured by sampling the cell culture supernatant after 5 days of incubation with cilengitide. The cell culture supernatants were added to a fluorophore-releasing reagent in a second 96-well assay plate and counted using a time-resolved fluorescence fluorimeter (excitation 340 nm; emission 615 nm).

Animal model and treatment application. Experiments performed in this study were approved by the governmental animal ethics committee (Regierungspräsidium Karlsruhe). Nude rats (RNU strain; Harlan-Winkelmann GmbH, Borchen, Germany) at the age of six weeks were housed in a specific pathogen-free environment in a mini barrier system under controlled conditions. For all procedures, rats were anesthetized using a mixture of nitrous oxide (1 l/min), oxygen (0.5 l/min) and isoflurane (1.5 vol%). MDA-MB-231 cells (10^5) were injected into the right superficial epigastric artery as described previously (24). Resulting bone metastases were observed exclusively in the femur, tibia and fibula of the right hind leg.

A total of 21 rats were treated with high dose (HD; 75 mg/kg) and 21 rats with low dose (LD; 25 mg/kg) cilengitide intraperitoneally five times per week, between days 1 and 30 after tumor cell inoculation. Animals that developed bone metastases after cilengitide treatment (HD, n=15 rats; LD, n=17 rats) were compared to the untreated control rats (n=17 rats) at days 30 and 35 after tumor cell inoculation using non-invasive imaging methods.

In vivo imaging and postprocessing. *In vivo* imaging of experimental bone metastases was performed on day 30 and 35 after the inoculation of cancer cells using a flat-panel volumetric computed tomograph (VCT; Volume CT; Siemens, Germany) and a 1.5 T clinical magnetic resonance scanner (Symphony; Siemens, Germany) as previously described (25). Briefly, VCT imaging was performed using the following parameters: tube voltage 80 kV, tube current 50 mA, scan time 51 sec, rotation speed 10 sec, frames per second 120,

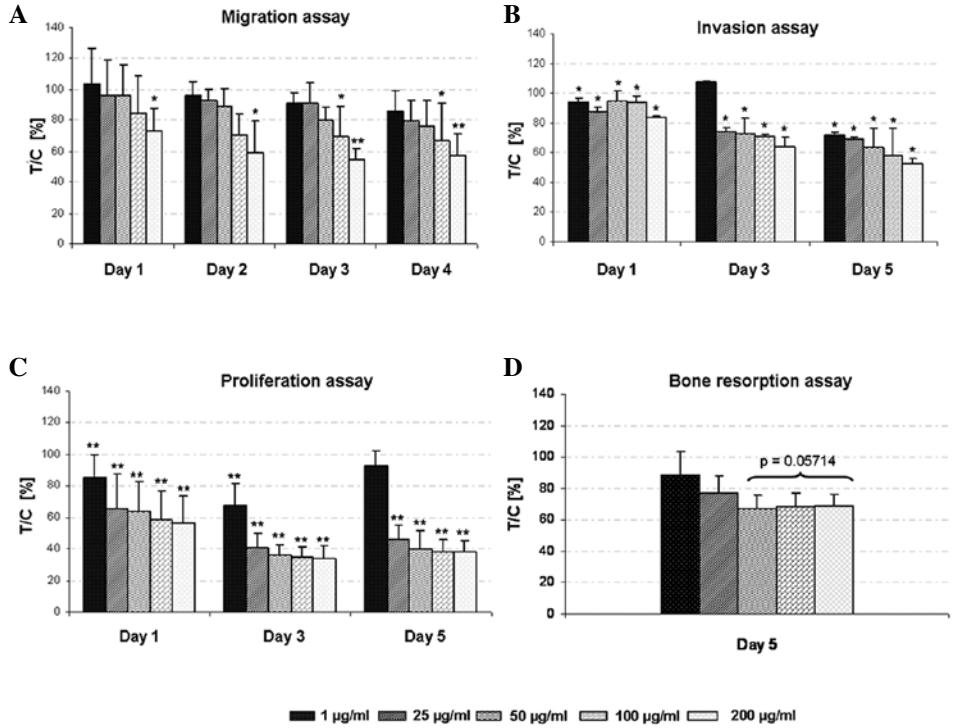

Figure 1. Migration (A), invasion (B) and proliferation (C) of MDA-MB-231 tumor cells as well as bone resorption of osteoclasts (D) in response to cilengitide *in vitro*. y-axis, mean treatment over control values in percent (T/C %); x-axis, incubation period of cilengitide. Error bars, standard deviation. Asterisks denote a significant difference by the two-sided Wilcoxon-test between cells incubated with cilengitide and control cells ($^{*}p<0.05$; $^{**}p<0.01$).

matrix 512 x 512, and slice thickness 0.2 mm. T2-weighted MR imaging was performed using a turbo spin echo sequence (orientation axial, TR 3240 msec, TE 81 msec, matrix 152 x 256, FOV 90 x 53.4 mm^2, slice thickness 1.5 mm, 3 averages, scan time 3:40 min). Dynamic contrast-enhanced MRI (DCE-MRI) was performed using a saturation recovery turbo flash sequence through the largest diameter of the tumor (orientation axial, TR 373 msec, TE 1.86 msec, matrix 192 x 144, FOV 130 x 97.5 mm, slice thickness 5 mm, measurements 512, averages 1, scan time 6:55 min). After 20 sec baseline 0.1 mmol/kg Gd-DTPA (Magnevist, Schering, Germany) was infused intravenously over a time period of 10 sec.

The volumes (ml) of the osteolytic lesions and the soft tissue components were determined from unenhanced VCT and MRI-acquired T2-weighted images using the Medical Imaging Interaction Toolkit (MITK, Heidelberg, Germany), respectively. DCE-MRI data were analyzed using the Dynalab software (Fraunhofer Mevis Research, Bremen, Germany) according to the two-compartment pharmacokinetic model of Brix to calculate the parameters amplitude A [(a.u.), associated with blood volume] and exchange rate constant k_{ep} [(1/sec), associated with vessel permeability] as previously reported (25).

Histology. On day 35 after tumor cell inoculation, animals were sacrificed. The lower limbs of each animal were excised and processed as described previously (25). For immunostaining, the sections (embedded in Technovit® 9100 NEU, Heraeus Kulzer, Germany) were incubated overnight with the following primary antibodies: rabbit anti-collagen IV pAB (1:50, Progen Biotechnik GmbH, Heidelberg, Germany) and mouse anti-smooth muscle actin (SMA) polyclonal antibody (1:400; Sigma Aldrich, St. Louis, MO). Sections were incubated with the secondary antibody for 1 h at room temperature as follows: Cy™ 2-conjugated donkey anti rabbit IgG and Texas Red® dye-conjugated goat anti-mouse IgG (1:50 and 1:100, respectively; Jackson Immunoresearch, Suffolk, UK). After a nuclear staining step with 4',6-diamidino-2-phenylindole (DAPI; Serva, Germany) sections were mounted in Fluoromount G (Southern Biotech, USA). Sections were examined using a Leica microscope (DMRE Bensheim, Germany) equipped with an adapted digital camera. Mean positive area fractions of SMA and collagen IV (%) as well as mean vessel diameters (μm) were determined from 4 representative animals of each group analyzing 10 fields of view chosen randomly using Analysis software (cell^{F}; Olympus Soft Imaging Solutions, Munich, Germany).

Statistical analyses. Treatment over control values in percent (T/C%) of the cilengitide-treated MDA-MB-231 cells were plotted vs. time after incubation. Comparison of the rate of tumor uptake of the bone metastases between the groups was performed using the χ^2 test. For each animal, absolute values for the osteolytic lesion and soft tissue component volumes, amplitude A as well as exchange rate constant k_{ep} were plotted vs. time after tumor cell inoculation. After quantitative histological analysis, the absolute values of the positive area fractions were compared. For statistical comparisons between the control and treatment groups, the absolute values were compared using the two-sided Wilcoxon-test; p-values <0.05 were considered significant.

Table I. Results of the *in vitro* study.

Assay	Concentration (in μg/ml)	Day 1	Day 2	Day 3	Day 4
Migration	1	103.9±23	96.3±9	90.9±7	85.7±14
	25	96.2±23	92.6±7	90.8±14	79.4±14
	50	96.2±19	88.9±12	80.1±8	76.2±16
	100	84.6±20	70.4±24	69.1±14[a]	66.7±14[a]
	200	73.1±15[a]	59.3±20[a]	54.5±7[b]	57.1±14[b]
		Day 1	Day 3	Day 5	
Invasion	1	93.7±2[a]	107.1±2	71.1±3[a]	
	25	87.9±4[a]	74.5±2[a]	68.9±1[a]	
	50	89.8±7[a]	73.7±6[a]	62.3±7[a]	
	100	89.2±6[a]	71.5±2[a]	58.0±10[a]	
	200	82.8±1[a]	64.2±4[a]	52.7±2[a]	
Bone resorption	1	-	-	88.5±15	
	25	-	-	76.9±11	
	50	-	-	66.9±9	
	100	-	-	68.4±9	
	200	-	-	69.1±7	
Proliferation	1	85.5±14[b]	67.4±14[b]	92.4±10	
	25	65.7±22[b]	40.9±9[b]	46.1±9[b]	
	50	63.9±19[b]	36.3±7[b]	39.9±12[b]	
	100	58.7±18[b]	35.1±7[b]	38.2±8[b]	
	200	56.7±17[b]	34.5±8[b]	38.0±8[b]	

Data are expressed as treatment over control values in percent (T/C%) ± standard deviation. [a]$p<0.05$ and [b]$p<0.01$, significant differences between MDA-MB-231 cells incubated with cilengitide in comparison to control cells (two-sided Wilcoxon-test).

Results

In vitro study

Migration. Following incubation of MDA-MB-231 cells with cilengitide for 4 days in a transwell migration model, less cells migrated in the treated (T) compared to the control (C) wells, and the ratio of the number of migrated cells of the treated to control cells (T/C%) on day 4 ranged from 86 (1 μg/ml, $p>0.05$) to 57 (200 μg/ml, $p<0.01$; Fig. 1A; Table I). Cells incubated with the highest concentration of 200 μg/ml cilengitide showed significantly reduced migration on all 4 days of the observation period compared to the controls ($p<0.05$).

Invasion. The number of invading cells incubated with cilengitide for 1, 3 and 5 days decreased significantly in a dose-dependent manner as compared to the controls (Fig. 1B; Table I). After cilengitide exposure, the T/C% values of the number of invaded cells from 107 (1 μg/ml, day 3; $p>0.05$) to 53 (200 μg/ml, day 5, $p<0.01$) were observed.

Proliferation. Incubation of MDA-MB-231 cells with cilengitide for 1, 3 or 5 days significantly decreased cell proliferation in a dose-dependent manner as determined by the MTT assay (Fig. 1C; Table I). T/C% values of the cells decreased from 92 (1 μg/ml, $p>0.05$) to 38 (200 μg/ml, $p<0.01$) after 5 days of incubation.

Bone resorption. Incubation of osteoclasts with cilengitide resulted in a decrease in the resorptive activity ranging from a T/C% value of 89 (1 μg/ml) to a T/C% value of 69 (200 μg/ml) after 5 days of incubation (Fig. 1D; Table I).

In vivo/ex vivo study

Morphological VCT and MRI. After tumor cell inoculation in nude rats, the tumor uptake in the bone metastases was not significantly different between the groups (controls, 77%; LD, 71%; HD, 81%; $p>0.05$, respectively). In the control animals the volumes for the osteolytic lesions (OL) and soft tissue components (SC) increased gradually between day 30 and day 35 (Figs. 2A and B, 3A and B; Table II). After therapy with cilengitide, OL and SC volumes were significantly reduced on days 30 and 35 in comparison to the untreated animals ($p<0.05$, respectively).

Dynamic contrast-enhanced MRI. Cilengitide treatment resulted in significantly decreased A values at days 30 and 35

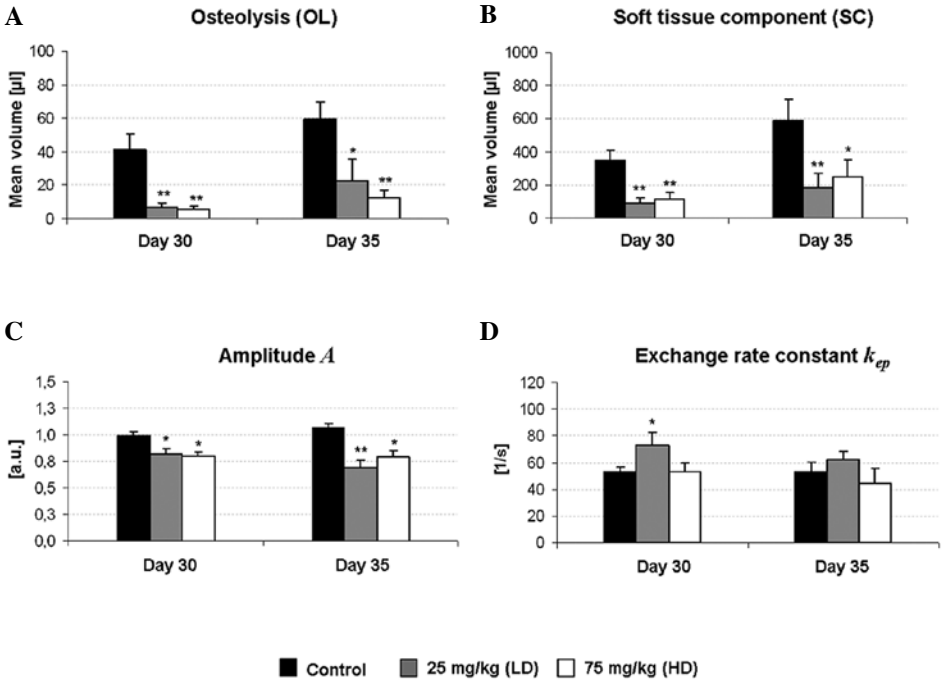

Figure 2. Volumetric analyses of the osteolytic lesions; OL (A) and soft tissue tumors; SC (B) as well as quantification of the mean relative values of parameters amplitude (C) and exchange rate constant k_{ep} (D) from experimental bone metastases. Comparison between the control and cilengitide-treated rats (low dose, LD and high dose, HD). y-axes: mean volumes of soft tissue components and osteolytic lesions as well as of DCE-MRI parameters A and k_{ep} (different scales); x-axes: days after cancer cell inoculation. Error bars, standard error. Asterisks denote a significant difference by the two-sided Wilcoxon test between treatment and control groups ($^{*}p<0.05$; $^{**}p<0.01$).

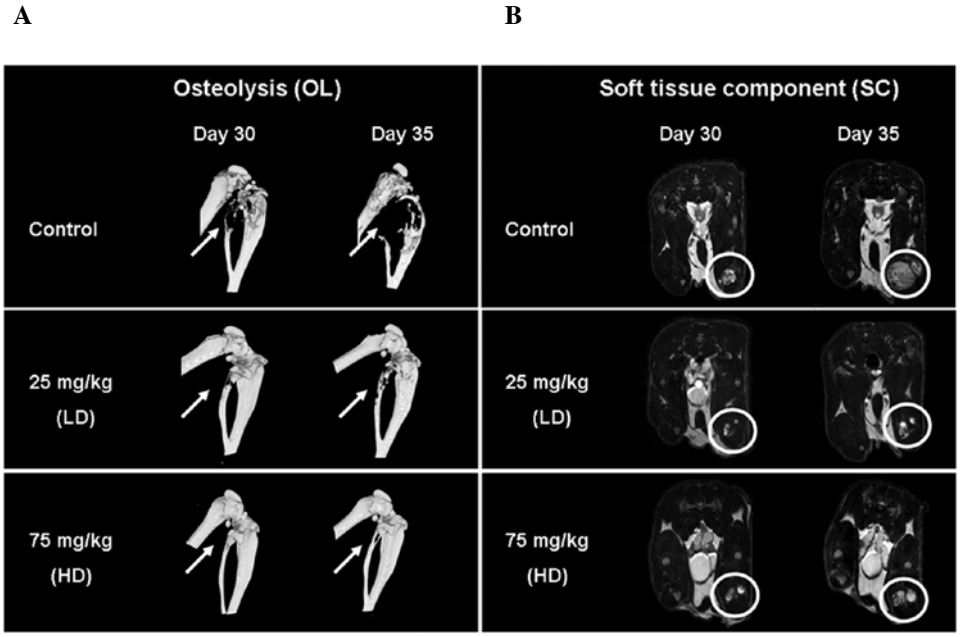

Figure 3. Morphological characteristics of experimental bone metastases in cilengitide-treated (low dose, LD and high dose, HD) and untreated animals. Osteolytic lesions; OL (A) and soft tissue tumors; SC (B) acquired by VCT and MRI, respectively, on days 30 and 35 after cancer cell injection. Representative VCT (3D bone surface reconstructions) and MR (axial T2-weighted sections) images of control (upper row) and treated (LD 25 mg/kg, middle row; HD 75 mg/kg, lower row) rats. Arrows indicate osteolytic lesions, circles delineate soft tissue tumors of the bone metastases.

after tumor cell inoculation ($p<0.05$, respectively; Figs. 2C and 4; Table II). Values for k_{ep} were significantly increased in the bone metastases after LD treatment in comparison to the untreated rats at day 30 ($p<0.05$), while HD treatment did not result in statistical differences between the groups (Fig. 2D).

Comparison between the treatment groups. No statistical difference was found between the treatment groups (LD and HD) for any measured parameters (tumor uptake rate, volumes of soft tissue components and osteolytic lesions as well as DCE-MRI parameters A and k_{ep}).

Table II. Results of the *in vivo* and *ex vivo* study.

In vivo	Group	Day 30	Day 35
VCT (volume of the osteolysis), μl	Control	41±9	59±10
	25 mg/kg (LD)	6.7±3[b]	23±13[a]
	75 mg/kg (HD)	5.5±2[b]	12.5±5[b]
MRI (volume of the soft tissue component), μl	Control	340±65	590±132
	25 mg/kg (LD)	90±29[b]	184±82[b]
	75 mg/kg (HD)	110±42[b]	250±104[a]
DCE-MRI (amplitude), a.u.	Control	0.9±0.04	1.1±0.04
	25 mg/kg (LD)	0.8±0.05[a]	0.7±0.07[b]
	75 mg/kg (HD)	0.8±0.04[a]	0.8±0.06[a]
DCE-MRI (exchange rate constant), 1/sec	Control	53.6±3	53.5±7
	25 mg/kg (LD)	73.0±10[a]	62.3±6
	75 mg/kg (HD)	53.0±7	44.2±11

Ex vivo	Collagen IV (%)	SMA (%)	SMA/ Collagen IV	Vessel diameter (μm)
Histology				
Control	4.9±0.9	4.5±0.8	0.9	17.7±1.2
25 mg/kg (LD)	7.9±1.2[a]	2.2±0.4[a]	0.3	8.3±0.4[b]
75 mg/kg (HD)	8.8±1.1[b]	2.8±0.8	0.3	9.2±0.4[b]

For *in vivo* experiments data are expressed as mean values ± standard error. For histology, values for collagen IV and smooth muscle actin (SMA) are expressed as positive area fractions in percent. (LD, 25 mg/kg; HD, 75 mg/kg) ([a]p<0.05; [b]p<0.01; two-sided Wilcoxon-Test).

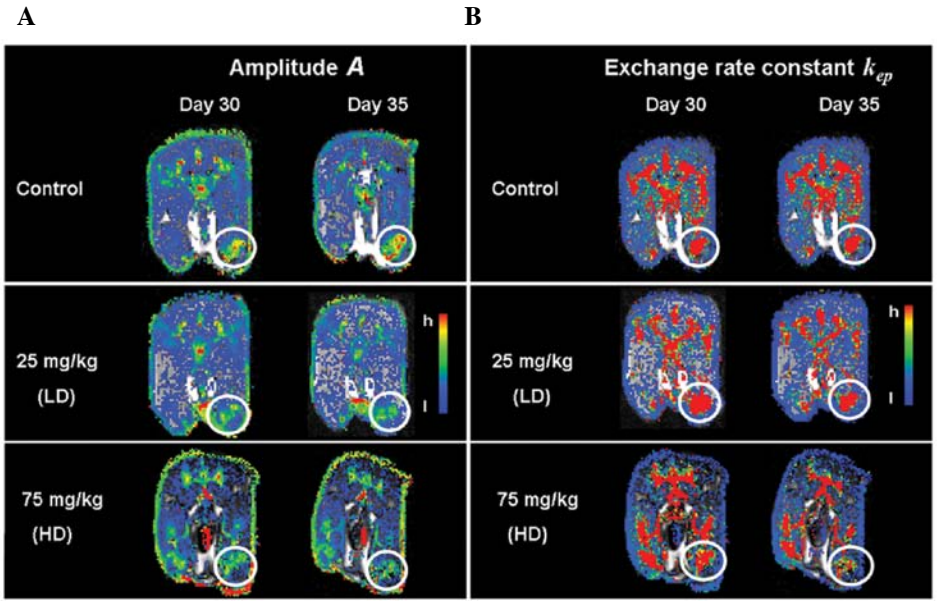

Figure 4. Color maps depicting DCE-MRI parameters of experimental bone metastases in the cilengitide-treated (low dose, LD and high dose, HD) and untreated animals. Amplitude A (A) and exchange rate constant k_{ep} (B) acquired by DCE-MRI, respectively, on day 30 and 35 after cancer cell injection. Red color denotes high (h) values for the given parameters, blue color denotes low (l) values. The same ranges were used to produce the images for the experimental and control animals. Circles delineate soft tissue tumors of bone metastases.

Histology. Immunofluorescent analysis indicated significantly increased mean area fractions of collagen IV (LD, p<0.05; HD, p<0.01) and significantly decreased mean area fractions of smooth muscle actin (SMA) (LD, p<0.05) in the treated animals (Fig. 5; Table II). The ratio of SMA and collagen IV (LD, 0.3; HD, 0.3; control, 0.9) was decreased in the animals after LD and HD treatment with cilengitide, and the mean vessel diameters in cilengitide-treated bone metastases (LD, 8.3 μm; HD, 9.2 μm) were significantly smaller than that in the control rats (17.7 μm, p<0.01; Figs. 5 and 6; Table II).

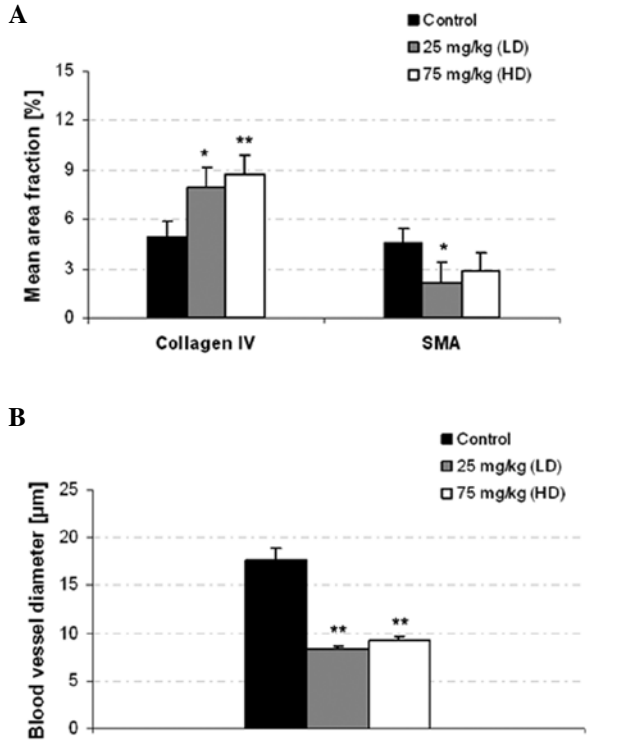

Figure 5. Quantification of the histological analysis of cilengitide-treated (low dose, LD and high dose, HD) and untreated experimental bone metastases. Values of fractional mean area stained for smooth muscle action (SMA) and collagen IV are expressed as percent total area examined (A) while the blood vessel diameters are presented as mean values in μm (B). (*p<0.05; **p>0.01; two-sided Wilcoxon test).

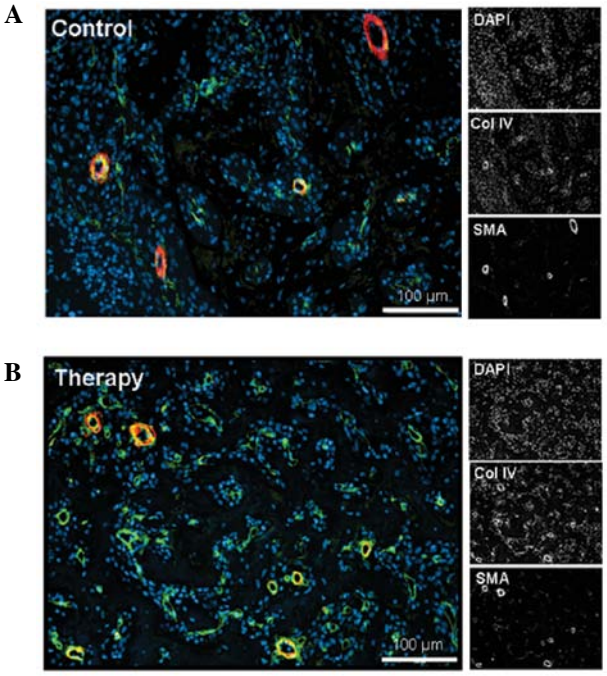

Figure 6. Immunofluorescent analysis of experimental bone metastases. Immunofluorescent analysis of experimentally induced bone metastases stained for SMA (red), collagen IV (green) and DAPI (blue) of a control rat (A) and a rat of the LD 25 mg/kg treatment group (B). Magnification, x20; bar, 100 μm.

Discussion

Current adjuvant treatment options for breast cancer patients are limited due to various factors including adverse effects of the administered drugs and the non-responsiveness of cancer cells. Novel therapeutic options able to effectively inhibit the development of metastases, including those of the skeleton, are urgently needed. The aim of the study was to assess the effects of $\alpha_v\beta_3/\alpha_v\beta_5$ integrin inhibition by cilengitide on early pathogenic steps of bone colonization including migration, invasion and proliferation of human MDA-MB-231 breast cancer cells as well as bone resorption, tumor growth and angiogenesis in experimentally induced bone metastases.

The present study reveals that adjuvant cilengitide treatment does not prevent metastasis to bone, but decreases tumor growth and osteolysis, and induces vessel remodelling in developing experimental skeletal metastases. As imaged by VCT, cilengitide treatment of nude rats resulted in a significant inhibition of osteolysis, which is in good agreement with the decreased osteoclast activity we observed *in vitro* upon incubation with cilengitide. Carron *et al* (26) reported a reduction in bone resorptive activity of osteoclasts *in vitro* after the inhibition of $\alpha_v\beta_3$ integrin, and several groups have demonstrated a decrease in bone resorption in breast cancer bone metastasis after inhibition of $\alpha_v\beta_3$ (27,28). As $\alpha_v\beta_3$ is expressed at high levels by osteoclasts it can be assumed that the inhibition of this integrin is primarily responsible for the observed anti-resorptive effect during bone colonization (29).

Furthermore, adjuvant cilengitide treatment was found to significantly reduce volumes of soft tissue tumors in experimental bone metastases. In line with this observation, our data showed that $\alpha_v\beta_3/\alpha_v\beta_5$ inhibition by cilengitide resulted in a significant decrease in proliferation of MDA-MB-231 cells *in vitro*. Correspondingly, previous studies have suggested a direct anti-tumor activity of this compound (14,16,30) and the growth of well-established bone metastases was found to decrease by cilengitide (20). We previously confirmed that $\alpha_v\beta_5$ is the primary α_v integrin expressed in MDA-MB-231 cells suggesting that the anti-tumor effect occurred due to the inhibition of this integrin rather than $\alpha_v\beta_3$ (20). However, the observed reduction in soft tissue component volumes after adjuvant cilengitide treatment may also be a consequence of the anti-angiogenic effect resulting from the inhibition of $\alpha_v\beta_3$ and $\alpha_v\beta_5$ on the endothelial of tumor vessels (14).

Concerning the effect of cilengitide on vascularization, we observed that adjuvant cilengitide treatment impaired vascular development, compatible with an anti-angiogenic effect during bone colonization. Non-invasive imaging displayed a decrease in the DCE-MRI-derived parameter associated with the relative blood volume (amplitude A) and an increase of the parameter associated with vessel permeability (exchange rate constant k_{ep}) in bone metastases. Immunohistological analysis revealed a decrease in the mean vessel diameter and SMA/collagen IV ratio in cilengitide-treated rats, which is in good agreement with DCE-MRI findings. These results are compatible with a decrease in blood volume due to smaller and partly non-functional blood vessels, and an increase in vessel permeability after adjuvant cilengitide treatment, e.g. due to the loss of intercellular contacts of endothelial cells

(31). We previously showed that cilengitide treatment resulted in corresponding changes in DCE-MRI parameters A and k_{ep} in well-established bone metastases (20). Our present results therefore, indicate that cilengitide not only alters already existing blood vessels, but also inhibits newly developing vascularization in bone marrow. In fact, recent studies have reported that $\alpha_v\beta_3$ and $\alpha_v\beta_5$ appear to be selectively expressed on growing vessels (32,33).

The mechanism of action of cilengitide on the early pathogenic steps of bone metastasis is currently unclear. Notably, the effect of cilengitide on proliferation *in vitro* exceeded the inhibition of migration and invasion of MDA-MB-231 breast cancer cells. The moderate reduction in migration and invasion, however, is in line with our finding that the uptake rate of bone metastases was not reduced after adjuvant cilengitide treatment. When comparing results from *in vitro* and *in vivo* experiments, the apparent percent reduction in lesion size in the hind legs of rats exceeded the inhibition of individual pathogenic processes *in vitro*, although the comparison is not rigorous. We therefore conclude that the effects of cilengitide on tumor cells, osteoclasts and vasculature are at least additive resulting in the observed decrease of skeletal lesion size.

Taken together, our data demonstrated a reduction in breast cancer cell migration, invasion and proliferation as well as osteoclastic bone resorption upon $\alpha_v\beta_3/\alpha_v\beta_5$ inhibition. Adjuvant cilengitide treatment in nude rats did not prevent bone metastasis formation, but reduced the volumes of soft tissue tumors and osteolyses of these lesions and induced vessel remodeling *in vivo*. In conclusion, cilengitide is a promising approach for the inhibition of bone metastasis formation during the processes of bone colonization in breast cancer and may serve as a combination partner for the adjuvant treatment of breast cancer patients in future clinical studies.

Acknowledgements

We thank Karin Leotta, Renate Bangert and Lisa Seyler for the excellent technical assistance as well as Simon Goodman and Horst Kessler for the valuable discussions. We furthermore thank the Deutsche Forschungsgemeinschaft (SFB-TR23 and SFB-TR79) and Merck-Serono for support.

References

1. Coleman RE: Metastatic bone disease: clinical features, pathophysiology and treatment strategies. Cancer Treat Rev 27: 165-176, 2001.
2. Gnant M: Bisphosphonates in the prevention of disease recurrence: current results and ongoing trials. Curr Cancer Drug Targets 9: 824-833, 2009.
3. Onishi T, Hayashi N, Theriault RL, Hortobagyi GN and Ueno NT: Future directions of bone-targeted therapy for metastatic breast cancer. Nat Rev Clin Oncol 7: 641-651, 2010.
4. Untch M, Möbus V, Janni W, *et al*: Therapie des primären Mammakarzinoms. In: Mammakarzinom Interdisziplinär. Kreienberg R, Möbus V, Jonat W and Kühn T (eds). Springer Verlag, Berlin, pp174-197, 2010.
5. Hynes RO: Integrins: bidirectional, allosteric signaling machines. Cell 110: 673-687, 2002.
6. Varner JA, Brooks PC and Cheresh DA: REVIEW: the integrin alpha V beta 3: angiogenesis and apoptosis. Cell Adhes Commun 3: 367-374, 1995.
7. Karadag A, Ogbureke KU, Fedarko NS and Fisher LW: Bone sialoprotein, matrix metalloproteinase 2, and alpha(v)beta3 integrin in osteotropic cancer cell invasion. J Natl Cancer Inst 96: 956-965, 2004.
8. Waltregny D, Bellahcene A, de Leval X, Florkin B, Weidle U and Castronovo V: Increased expression of bone sialoprotein in bone metastases compared with visceral metastases in human breast and prostate cancers. J Bone Miner Res 15: 834-843, 2000.
9. Arndt T and Arndt U: Integrin in angiogenesis: implications of tumor therapy. In: Cancer Therapy: Molecular Targets in Tumor-Host Interactions. Weber GF (ed). Horizon Bioscience, Norfolk, UK, 2005.
10. Varner JA: The role of vascular cell integrins alpha v beta 3 and alpha v beta 5 in angiogenesis. EXS 79: 361-390, 1997.
11. Rodan SB and Rodan GA: Integrin function in osteoclasts. J Endocrinol 154 (Suppl): S47-S56, 1997.
12. Harms JF, Welch DR, Samant RS, *et al*: A small molecule antagonist of the alpha(v)beta3 integrin suppresses MDA-MB-435 skeletal metastasis. Clin Exp Metastasis 21: 119-128, 2004.
13. Dechantsreiter MA, Planker E, Matha B, *et al*: N-Methylated cyclic RGD peptides as highly active and selective alpha(V) beta(3) integrin antagonists. J Med Chem 42: 3033-3040, 1999.
14. Nisato RE, Tille JC, Jonczyk A, Goodman SL and Pepper MS: alphav beta 3 and alphav beta 5 integrin antagonists inhibit angiogenesis in vitro. Angiogenesis 6: 105-119, 2003.
15. Patsenker E, Popov Y, Stickel F, *et al*: Pharmacological inhibition of integrin alphavbeta3 aggravates experimental liver fibrosis and suppresses hepatic angiogenesis. Hepatology 50: 1501-1511, 2009.
16. Mulder WJ, Castermans K, van Beijnum JR, *et al*: Molecular imaging of tumor angiogenesis using alphavbeta3-integrin targeted multimodal quantum dots. Angiogenesis 12: 17-24, 2009.
17. Pecheur I, Peyruchaud O, Serre CM, *et al*: Integrin alpha(v)beta3 expression confers on tumor cells a greater propensity to metastasize to bone. FASEB J 16: 1266-1268, 2002.
18. Reardon DA, Nabors LB, Stupp R and Mikkelsen T: Cilengitide: an integrin-targeting arginine-glycine-aspartic acid peptide with promising activity for glioblastoma multiforme. Expert Opin Investig Drugs 17: 1225-1235, 2008.
19. Reardon DA, Fink KL, Mikkelsen T, *et al*: Randomized phase II study of cilengitide, an integrin-targeting arginine-glycine-aspartic acid peptide, in recurrent glioblastoma multiforme. J Clin Oncol 26: 5610-5617, 2008.
20. Bäuerle T, Komljenovic D, Merz M, Berger MR, Goodman SL and Semmler W: Cilengitide inhibits progression of experimental breast cancer bone metastases as imaged non-invasively using VCT, MRI and DCE-MRI in a longitudinal in vivo study. Int J Cancer 128: 2453-2462, 2011.
21. Adwan H, Bäuerle T, Najajreh Y, Elazer V, Golomb G and Berger MR: Decreased levels of osteopontin and bone sialoprotein II are correlated with reduced proliferation, colony formation, and migration of GFP-MDA-MB-231 cells. Int J Oncol 24: 1235-1244, 2004.
22. Bäuerle T, Peterschmitt J, Hilbig H, Kiessling F, Armbruster FP and Berger MR: Treatment of bone metastasis induced by MDA-MB-231 breast cancer cells with an antibody against bone sialoprotein. Int J Oncol 28: 573-583, 2006.
23. Kenig S, Alonso MB, Mueller MM and Lah TT: Glioblastoma and endothelial cells cross-talk, mediated by SDF-1, enhances tumour invasion and endothelial proliferation by increasing expression of cathepsins B, S, and MMP-9. Cancer Lett 289: 53-61, 2010.
24. Bäuerle T, Adwan H, Kiessling F, Hilbig H, Armbruster FP and Berger MR: Characterization of a rat model with site-specific bone metastasis induced by MDA-MB-231 breast cancer cells and its application to the effects of an antibody against bone sialoprotein. Int J Cancer 115: 177-186, 2005.
25. Bäuerle T, Merz M, Komljenovic D, Zwick S and Semmler W: Drug-induced vessel remodeling in bone metastases as assessed by dynamic contrast enhanced magnetic resonance imaging and vessel size imaging: a longitudinal in vivo study. Clin Cancer Res 16: 3215-3225, 2010.
26. Carron CP, Meyer DM, Engleman VW, *et al*: Peptidomimetic antagonists of alphavbeta3 inhibit bone resorption by inhibiting osteoclast bone resorptive activity, not osteoclast adhesion to bone. J Endocrinol 165: 587-598, 2000.
27. Nakamura I, Duong lT, Rodan SB and Rodan GA: Involvement of alpha(v)beta3 integrins in osteoclast function. J Bone Miner Metab 25: 337-344, 2007.

28. Zhao Y, Bachelier R, Treilleux I, *et al*: Tumor alphavbeta3 integrin is a therapeutic target for breast cancer bone metastases. Cancer Res 67: 5821-5830, 2007.
29. Vaananen HK, Zhao H, Mulari M and Halleen JM: The cell biology of osteoclast function. J Cell Sci 113: 377-381, 2000.
30. Mitjans F, Meyer T, Fittschen C, *et al*: In vivo therapy of malignant melanoma by means of antagonists of alphav integrins. Int J Cancer 87: 716-723, 2000.
31. Oliveira-Ferrer L, Hauschild J, Fiedler W, Bokemeyer C, Nippgen J, Celik I and Schuch G: Cilengitide induces cellular detachment and apoptosis in endothelial and glioma cells mediated by inhibition of FAK/src/AKT pathway. J Exp Clin Cancer Res 27: 86, 2008.
32. Brooks PC, Montgomery AM, Rosenfeld M, Reisfeld RA, Hu T, Klier G and Cheresh DA: Integrin alpha v beta 3 antagonists promote tumor regression by inducing apoptosis of angiogenic blood vessels. Cell 79: 1157-1164, 1994.
33. Brooks PC, Clark RA and Cheresh DA: Requirement of vascular integrin alpha v beta 3 for angiogenesis. Science 264: 569-571, 1994.